A model for the basic plasma parameter profiles and the force exerted by fireballs with non-isothermal electrons

J. Gruenwald, J. Kovačič, B. Fonda, and T. Gyergyek

Citation: Physics of Plasmas **25**, 113508 (2018); doi: 10.1063/1.5054369
View online: https://doi.org/10.1063/1.5054369
View Table of Contents: http://aip.scitation.org/toc/php/25/11
Published by the American Institute of Physics

PHYSICS OF PLASMAS 25, 113508 (2018)

A model for the basic plasma parameter profiles and the force exerted by fireballs with non-isothermal electrons

J. Gruenwald,[1,a)] J. Kovačič,[2,3] B. Fonda,[3] and T. Gyergyek[2,3]
[1]Gruenwald Laboratories, Taxberg 50, 5660 Taxenbach, Austria
[2]Faculty of Electrical Engineering, University of Ljubljana, Tržaška cesta 25, SI-1000 Ljubljana, Slovenia
[3]Jozef Stefan Institute, University of Ljubljana, Jamova 39, SI-1000 Ljubljana, Slovenia

(Received 31 August 2018; accepted 24 October 2018; published online 9 November 2018)

As discovered in recent work, plasma fireballs have the ability to exert considerable force onto ions and neutrals and, hence, induce macroscopic gas flows. This property makes them interesting objects for fundamental scientific research. Furthermore, there are also the possibilities for applications in the field space propulsion. As there is a lack of fundamental understanding of these plasma phenomena, this article aims to enhance the physical knowledge of fireballs by presenting a mathematical model for the calculation of the force that can be provided by them. It will be shown that all the main plasma parameters such as the plasma potential and the electron density can be derived completely with the knowledge of the potential of the electrode and the radial electron temperature profile. The calculations show very good agreement with the experimental data if two species of electrons (i.e., fast and slow) are considered. Both electron populations have different temperature profiles as is shown with measurements. Furthermore, it will be demonstrated that the potential drop throughout the fireball is much larger than previously thought and that this larger potential drop can considerably contribute to the acceleration of ions in the double layer. This mechanism makes it more likely that the force exerted by the fireball is rather caused by heating of the neutrals via collisions with those accelerated ions and the high energetic ions themselves than by collisions between fast electrons and neutrals. *Published by AIP Publishing.*
https://doi.org/10.1063/1.5054369

I. INTRODUCTION

Fireballs (FBs) are spherical, highly luminous regions in a comparably thin surrounding background plasma, which are bounded by a double layer (DL). They were first reported by Lehmann at the beginning of the last century.[1] It was discovered some years ago by Stenzel *et al.*[2] that FBs are capable of producing macroscopic flows in the surrounding gas. It was argued by the latter authors that these gas flows were induced by fast electrons that heat the neutrals. This pioneering work was later supplemented by a theoretical model by Makrinich and Fruchtman[3] along with the partial comparison of the theoretical data with measurements. The aforementioned model is a good starting point for theoretical investigations. However, there is still room for improvement. Specifically, the assumption of isothermal electrons made in Ref. 3 is a simplification that is not congruent with experimental data, obtained by different authors such as Rubens and Henderson[4] who measured differences in T_e of up to 250% between the interior of a FB and the bulk plasma. A more recent experimental study, which clearly shows that the assumption of isothermal electrons only holds within the FB and outside the double layer (but with very different values), was conducted by Weatherford *et al.*[5] However, if only isothermal electrons are considered, the behavior of the electrons in the boundary region of the FB, which is formed by the DL, is completely neglected. In Sec. III, the model by Makrinich *et al.* is generalized to FBs with non-isothermal electrons, and the results are compared with experimental data. Additionally, it will be shown that the potential drop throughout the fireball is much larger than it would be the case with only one electron species and that this larger potential drop can considerably contribute to the acceleration of ions in the double layer. The calculations presented in this work are based on a simplified analytic model, which neglects kinetic effects in the plasma but still yields results that are in good agreement with the available experimental data.

II. EXPERIMENTAL SETUP

The experimental results, which were used to support the following mathematical model, were obtained in a linear, magnetized plasma machine that produces the plasma with a hot wire cathode and has an axial magnetic field for enhanced confinement. This device is described in more detail elsewhere.[6] However, a schematic overview of the machine is shown in Fig. 1.

The magnetic field was held as small as possible (11 mT) to minimize anisotropy effects, and the radial plasma parameter profiles were measured with Langmuir and emissive probes. Both probe heads were made of thoriated tungsten with a length of 5 mm and a diameter of 75 μm. The probes were orientated perpendicular to the magnetic field lines, and the data evaluation was conducted according to standard probe theory. The magnitude of the magnetic field is also considered low enough not to influence the probe measurements.[7] The experiments were conducted

[a)]E-mail: jgruenwald@gmx.at

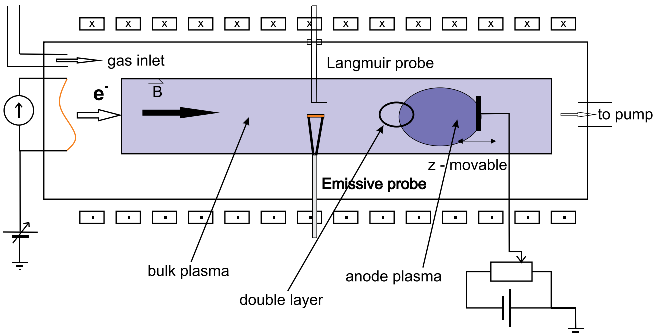

FIG. 1. Sketch of the Ljubljana magnetized plasma machine with the additional anode and the FB.

in argon 5.0 at a pressure of 10^{-2} mbar. The discharge current was 2.4 A at a discharge voltage of 50 V.

As depicted in Fig. 2 within the FB, a second population of electrons with considerably higher temperature evolves inside the double layer surrounding the FB. The applied potential on the anode was 30.9 V with respect to ground at a maximum input current of 0.3 A.

This gives already a hint that the potential drop in the double layer accelerates the ions produced in the FB, which then heat the neutrals due to inelastic collisions rather than the electrons. The magnitude of the temperature drop also fits to the measurements of Stenzel *et al.* who observed ballistic ions leaving a pulsed FB with kinetic energies of 8.6 to 12.9 eV under very similar experimental conditions.[8] It has to be noted that there are indeed isothermal electrons present but at very low temperature which cannot account either for the generation of fast ions that are observed in the FB or for the neutral gas heating.

III. COMPARISON BETWEEN THE MODEL AND THE EXPERIMENT

As can be seen in Fig. 2, the electron temperature profile can be approximated with a logistic function that has the general form

$$T_e(r) = A + \frac{L - A}{1 + \exp(-k(r - r_0))}, \tag{1}$$

where A, L, k, and r_0 are usually fit parameters. However, in this context, they refer to the following physical quantities: A is the electron temperature in the bulk (far from the FB), L is the maximum value of T_e in the center (near the electrode), k is the steepness, and r_0 is the midpoint of the curve. For the sake of simplicity and without loss of generality, A is set to be 0 and L is from here on defined as the maximum electron temperature with respect to T_e in the bulk (L = 9.1 eV). As shown later, the hot electron population is less dense. This leads to a larger scattering of the data points for the hot electrons although 10 measurements were averaged for each acquisition. However, the overall accuracy of the Langmuir probe measurements is about 10%. Both the plasma potential ϕ_{pl} and the electron temperature can be connected under the assumption of quasi neutrality ($n_{e,c} + n_{e,h} = n_e \approx n_i = n$) and a Maxwellian velocity distribution via[9,10]

$$\phi_{pl} = \frac{T_e}{2} \cdot \left[1 + ln\left(\frac{2M_i}{\pi m_e}\right)\right] - \phi_{FB}, \tag{2}$$

where ϕ_{FB} is the potential on the FB anode inside the FB, while its value is zero outside the FB where the electrode potential is already shielded from the background plasma. The indices "h" and "c" denote the contributions from the hot and cold electrons, respectively. Due to the superposition principle, this can be done separately for the hot and cold electrons with their individual temperature profiles.

Two typical electron energy distribution functions (EEDF) from the hot and cold population are shown in Fig. 3.

The distribution functions have been obtained by the second derivative of the Langmuir probe traces. The probe traces have been smoothed with a Savitzky–Golay filter with the optimal parameters to minimize the error lined out in Ref. 11. It can be seen that the EEDF for both electron species are Maxwellian. However, there is some slight deviation in the distribution function for the cold electrons, which can be explained by the larger mean free paths at smaller electron energies.

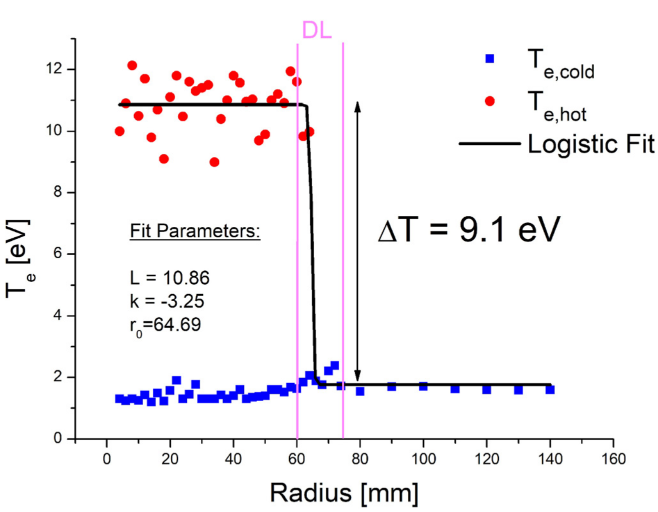

FIG. 2. Double layer (pink) formed between 60 and 75 mm and measured radial temperature profiles of the cold (blue) and hot (red) electrons with a logistic fit (black) as obtained with the listed fit parameters.

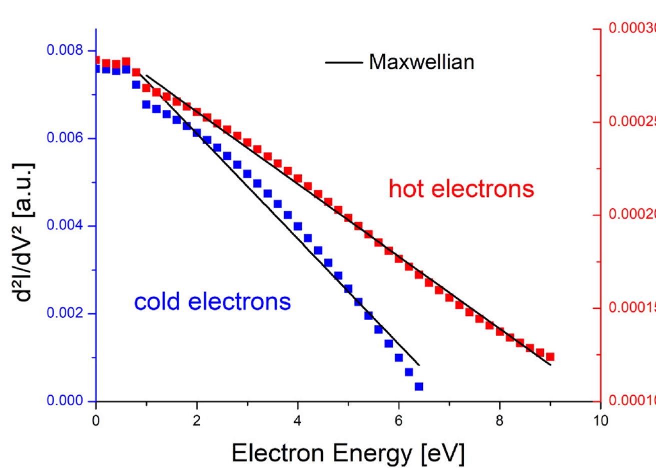

FIG. 3. Typical EEDF taken at positions 40 and 100 mm. Savitzky–Golay parameters: polynomial order: 6 and data points: 191.

The results for ϕ_{pl} are depicted in the graph (Fig. 4), which shows a comparison between the plasma potential profiles calculated according to Eq. (2) and the equation suggested by Makrinich and Fruchtman.[3] The black squares in Fig. 4 denote the actually measured data. The plot contains the data for the hot electrons (red line), the cold electrons (blue line), and the sum of both contributions with the potential of the FB electrode (30.9 V) subtracted as described by Eq. (2) (black line). It is clearly visible that both species of electrons, i.e., the hot and the cold population, have to be taken into account in order to obtain the correct plasma potential profile. This is despite the fact that the majority of electrons in the FB plasma are part of the cold, isothermal population.

The best agreement between the experimental data and the simulated curve can only be obtained if the cold and hot electrons and the potential on the anode are taken into account properly. Nevertheless, it has to be noted that the temperature for the hot electrons was set to be zero outside the FB as the only experimentally observed population in this region is the one consisting of cold electrons. Hence, for radial positions larger than 66 mm, the hot electrons are omitted. However, for obtaining the blue line, isothermal cold electrons were assumed, while for the red line, the two different temperatures of the electrons within and outside the FB have been regarded. Using Eq. (2) yields a potential drop of around 30 V in the DL, which is around 6 times higher than the potential drop calculated with the conventional formula (4.8 V).[3] This again strengthens the claim that ions can indeed gain enough kinetic energy in the potential drop, which is then available for neutral gas heating via inelastic collisions. The drop in the plasma potential of around 30 V indicates the possibility of the creation of Ar^{2+} ions as the second ionization potential of argon is 28.6 eV, but these species are neglected here for simplicity. It has also to be noted that the plasma potential inside the FB is slightly higher than the potential on the electrode, which is explained by the rapid loss of electrons on the anode surface along with the efficient production of positively charged ions. The derivative of Eq. (2) allows us to calculate the E-field for the hot and cold electrons

$$E_{h,c} = \nabla \phi_{pl,h,c} = \frac{\partial}{\partial r} \phi_{pl,h,c}. \tag{3}$$

The contribution from each electron species to the E-field was calculated from Eq. (3), and the results are depicted in Fig. 5.

It can be seen that the cold electrons only have a marginal influence on the total electric field between the FB anode and the background plasma since their contribution only shows some minor fluctuations around the zero line. The hot electrons, on the other hand, display E-field fluctuations of several thousand V/m with a strong maximum value of around 10 kV/m in the DL around the FB. However, it has to be stressed that the large distortions of the E-field inside the FB are not physical; they are due to the limitations in the probe evaluation techniques in combination with the numerical derivation of the data curves. Since the electron temperature was determined from the semi-log plot of the probe traces, even small errors may appear as large fluctuations. Nevertheless, it can be concluded that the cold electrons alone cannot be responsible for the large E-field variation within the double layer as their contribution to the electrical field is about three orders of magnitude too small compared to the calculation from the measured plasma potential.

With the knowledge of the plasma potential and the electron temperature profiles of both species, the electron density profiles can be calculated in the following manner: First, the general momentum equation for the electrons is needed

$$-en_eE = \frac{\partial(n_eT_e)}{\partial r} = \frac{\partial n_e}{\partial r} \cdot T_e + \frac{\partial T_e}{\partial r} \cdot n_e. \tag{4}$$

It is evident that the assumption of non-isothermal electrons introduces an additional term into the momentum equation. Since the electric fields generated by the fast and slow

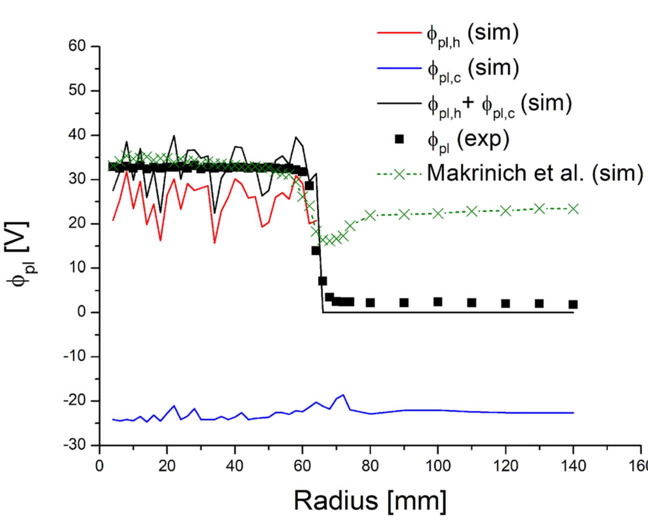

FIG. 4. Simulated radial plasma potential profile contributions of the hot (red) and cold (blue) electrons and their sum minus the FB electrode potential (black line), calculated with Eq. (2). They are compared with the measured radial profiles (black squares) and with the theoretical predictions from Ref. 3 (green crosses).

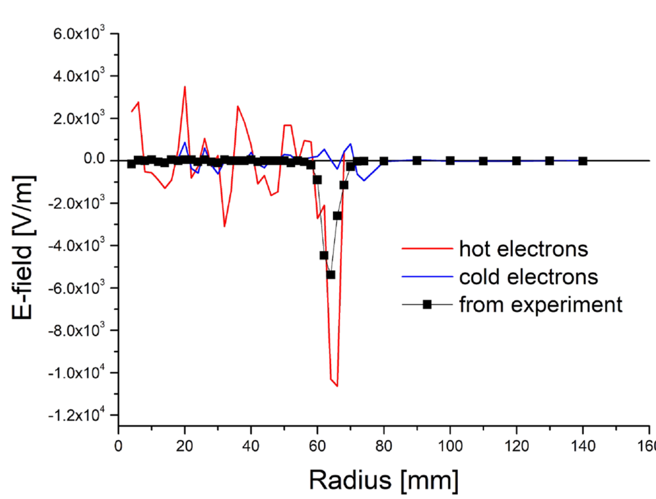

FIG. 5. Simulated contributions to the electric field from the cold (blue) and hot (red) electrons in comparison to the electric field calculated from the experimental values (black).

electrons can be superimposed, Eq. (4) can be treated separately for both electron species

$$-en_{e,c}(r)E_c(r) = \frac{\partial n_{e,c}}{\partial r} \cdot T_{e,c} \tag{5}$$

and

$$-en_{e,h}E_h = \frac{\partial n_{e,h}}{\partial r} \cdot T_{e,h} + \frac{\partial T_{e,h}}{\partial r} \cdot n_{e,h}. \tag{6}$$

It has to be noted that $T_{e,c}$ in Eq. (5) is constant in accordance with the measured data, depicted in Fig. 2. Thus, Eq. (5) yields the solution for the density of slow electrons

$$\begin{aligned} n_{e,c} &= n_{c,0} \cdot \exp\left[-\frac{e}{T_{e,c}}\int_1^r E(\zeta)d\zeta\right] \\ &= n_{c,0} \cdot \frac{\exp\left[\frac{e}{T_{e,c}}\phi_{pl,c}(1)\right]}{\exp\left[\frac{e}{T_{e,c}}\phi_{pl,c}(r)\right]}, \end{aligned} \tag{7}$$

where $n_{c,0}$ denotes the density of cold electrons at the surface of the FB electrode and $\phi_{pl,c}$ is the plasma potential contribution from the cold electrons. The hot electron density is determined via Eq. (6). Using the general derivation rules for the logistic function, the spatial derivative of the electron temperature is then given by

$$\frac{\partial T_{e,h}}{\partial r} = T_{e,h} \cdot (1 - T_{e,h}) \tag{8}$$

and

$$\frac{\partial^2 T_{e,h}}{\partial^2 r} = T_{e,h} \cdot (1 - T_{e,h}) \cdot (1 - 2T_{e,h}). \tag{9}$$

For the following mathematical treatment, also the momentum equation for the ions

$$m_i \nu \Gamma_i = n_i e E \tag{10}$$

along with the continuity equation

$$\frac{1}{r^2}\frac{\partial}{\partial r}(r^2\Gamma_i) = S \tag{11}$$

is applied.[3] Here, Γ_i denotes the ion particle flux density and S is the source term that takes into account particle generation via impact ionization within the FB. As the cold electrons have too little energy to ionise, these calculations regard only the hot electrons. For moderate gas and electron densities, the source term is proportional to the neutral gas density N and the electron impact ionization rate β ($\sim 10^{-16}\,\mathrm{m^3/s}$ for Ar[12])

$$S = \beta N n_{e,h}. \tag{12}$$

Additionally, a constant collision frequency of the neutrals in the gas is assumed

$$\nu = \sigma N v_{th}, \tag{13}$$

with the ion-atom cross section σ ($4 \times 10^{-17}\,\mathrm{m^2}$ for Ar atoms according to Phelps *et al.*[13]) and the thermal velocity of the gas particles v_{th}. Under the assumption of quasi neutrality, (4) and (10) are combined to get

$$-\frac{\partial(n_{e,h}T_{eh})}{\partial r} = m_i \nu \Gamma_i, \tag{14}$$

which yields in connection with Eqs. (11)–(13) the following spherical diffusion equation:

$$-m_i\sigma\beta N^2 v_{th} n_{e,h} = K \cdot n_{e,h} = \frac{1}{r^2}\frac{\partial}{\partial r} \cdot \left[r^2 \cdot \frac{\partial(n_{e,h}T_{e,h})}{\partial r}\right]. \tag{15}$$

Here, K was used as an abbreviation for all the constant prefactors in front of the hot electron density. It has to be noted that strictly speaking, the criterion of quasineutrality is violated in the region of the double layer (DL) surrounding the FB plasma, but the thickness of the DL is very small compared to the spatial dimensions of the FB and the surrounding plasma that it can be neglected without introducing too large errors in the calculations. Introducing the abbreviations T' and n' for the spatial derivatives and solving the r.h.s. of Eq. (15), the following differential equation is obtained for the plasma density n:

$$n''Tr + n'(2T + 2T'r) + n(2T' + rT'' - K) = 0. \tag{16}$$

Calculating K with parameters that are typical for FB discharges (i.e., covering also the parameter range of the experiments presented herein), namely, $m_i = 6.6 \times 10^{-26}$ kg for Ar and $N = 2.4 \times 10^{20}\mathrm{m^{-3}}$ for an ideal gas at room temperature and a pressure of 10^{-2} mbar yields $\sim 6 \times 10^{-15}\mathrm{m^3\,kg/s^2}$. The thermal energy of the argon neutrals, which is needed for the calculation of K, was obtained via

$$v_{th} = \sqrt{\frac{8kT}{\pi m_i}} = 400\,\mathrm{m/s}. \tag{17}$$

Hence, this term is neglected in the solution of Eq. (16). Equation (16) indicates that

$$(nTr)'' = 0, \tag{18}$$

which has the general solution for $T, r \neq 0$

$$n(r) = \frac{Br + C}{Tr} = \frac{B}{T} + \frac{C}{Tr}. \tag{19}$$

Since the current continuity $j = en_e v_e$ has to be fulfilled for the whole plasma, the following condition is satisfied:

$$n(0)T(0) = n(\infty)T(\infty). \tag{20}$$

This can only hold if the solution for n(r) has no linear dependence on r. Hence

$$\frac{B}{Tr} \stackrel{!}{=} 0 \leftrightarrow B = 0. \tag{21}$$

The particular solution is obtained by the definition of suitable boundary conditions, i.e.,

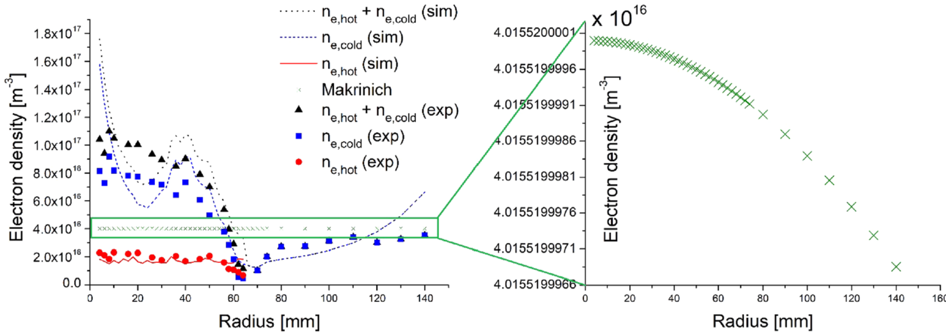

FIG. 6. Left: Simulated and measured radial density profiles of the hot electrons, calculated with Eq. (23) (red), the cold electrons, calculated with Eq. (7), and their sum in comparison to the formula derived after equation (11) in Ref. 3 (green crosses). Right: A magnification of the density profile simulated with Markinich's equation.

$$n(0) = n_{h,0} = \frac{B}{T_{e,h}(r=0)} = \frac{2}{L} \cdot B. \tag{22}$$

Thus

$$n(r) = n_{h,0} \cdot \frac{L}{2} \cdot \frac{1}{T_{e,h}(r)}. \tag{23}$$

The results of Eqs. (7) and (23) are shown in Fig. 6 in direct comparison with the measured density profiles, where the red, blue, and black symbols depict the measured density profiles for the different species. The dashed lines represent the calculated values. The shapes of the profiles are in good agreement except for the range in close vicinity to the FB electrode where some more complicated physical processes are possibly going on. However, most of the discrepancies can be explained either by the accuracy of the probe data evaluation or by the simplifications that were made during the calculations [e.g., omitting the constant K in Eq. (15)]. It also has to be noted that there seems to be a divergence in the cold electron density profile for larger radii. This is purely due to the structure of Eq. (7) where even small inaccuracies contribute exponentially to the density profile calculations. The same holds for the seemingly diverging $n_{e,c}$ profiles close to the electrode surface, where the distortions of the plasma potential profile are relatively large. In comparison, the use of the equation presented by others[3] (green dashed line) yields a profile that is only marginally dependent on the radial position with a kind of average value for the electron density. In fact, the results for n_e calculated via Eq. (11) from Ref. 3 only vary in the 9th digit behind the comma as depicted on the right hand side of Fig. 6.

With these results, the ion flux through the surface of the FB can be written as

$$\Gamma_R = 4\pi r^2 \Gamma_i = -\frac{4\pi r^2}{m_i \sigma N v_T} \cdot [n'T + nT'], \tag{24}$$

while the total outward force on the ions is obtained by integrating the momentum equation

$$F_{tot} = -4\pi \int_0^r [n'T + nT']\tilde{r}^2 d\tilde{r}. \tag{25}$$

Figure 7 displays the simulated total force exerted of a FB with radius r along with the ion flux outwards the FB.

It can readily be seen that the ion flux reaches its maximum at the edge of the FB. Furthermore, the total force exerted by the ions displays a very strong increase inside and shortly outside the double layer, which surrounds the FB. This is also a strong indication that at least some of the ion thrust is due to electrostatic acceleration in the sheath. The total force of the FB reaches a value of around 8 mN, which seems astonishingly high; however, it has to be emphasized that this is the value acting outwards the FB in all directions. The area of a FB with a radius of 70 mm is 615.8 cm^2, which yields a force per unit area of roughly 1.3×10^{-5} N/cm^2. This corresponds to a force of 48.8 μN on a 3.76 cm^2 pendulum as it was used by Makrinich and Fruchtman.[3] under very similar experimental conditions. This number is in excellent agreement with the value obtained by those authors who measured the force to be 46 ± 5 μN.

Consequently, the force exerted on a single ion at the edge of the FB (where r = R) is given by

$$\frac{F_{tot}}{\Gamma_R} = \frac{m_i \sigma N v_T}{R^2} \cdot \frac{\int_0^R [n'T + nT']\tilde{r}^2 d\tilde{r}}{[n'T + nT']}. \tag{26}$$

The value of the force per ion in the center of the DL, which was numerically calculated from Eq. (26), is 9.1×10^{-18} N. However, the maximum force on a single ion is 6×10^{-16} N/ion and is found to be about 1 cm outside the DL, as shown in Fig. 8: One can see from the semi-log plot of the force on a single ion that there is a strong increase in force inside the DL from 2×10^{-18} to 3.7×10^{-17}. This indicates that the main acceleration of the ions is indeed happening in the DL that surrounds the FB. It has to be noted at this

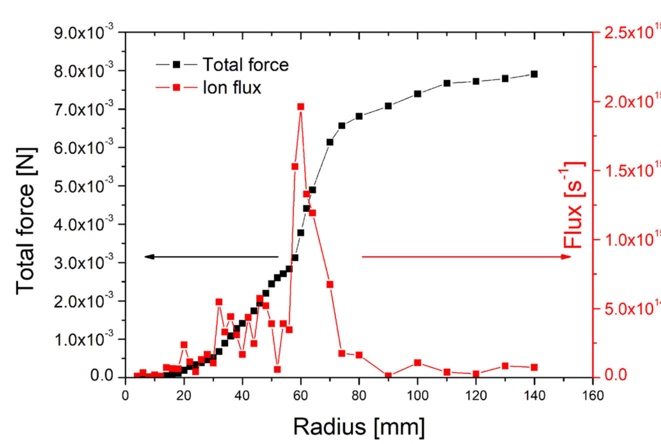

FIG. 7. Simulated total force exerted by the FB (black) and the simulated ion flux in dependence of the radius (red).

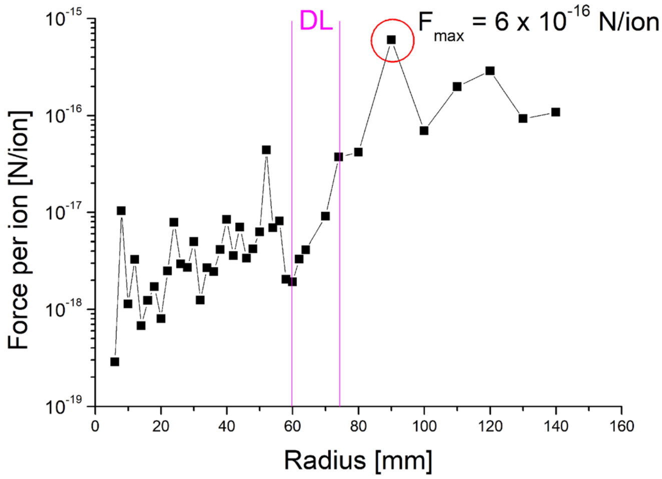

FIG. 8. Simulated force on a single ion as a function of the distance to the FB electrode on a semi-log scale.

point that besides this, there is also another argument that makes the neutral gas heating due to electron-neutral collisions, which was suggested by former authors, very unlikely. To elaborate this, the mean free path of electron-neutral collisions has to be taken into account[14]

$$\lambda_{mfp} = \frac{v_{e,th}}{N\langle \sigma v \rangle}, \tag{27}$$

where $v_{e,th}$ is the average thermal velocity of the electrons and $\langle \sigma v \rangle$ is the reaction rate coefficient for elastic neutral-electron scattering. The former entity can be calculated analogous to Eq. (17) with the electron mass $m_e = 9.1 \times 10^{-31}$ kg. This yields in accordance with the data from Ref. 15 an electron mean free path (for $T_e = 8\,\text{eV}$) in Ar of around 10 cm for the experiments described herein. As this is on the order of (or even larger than) the diameter of the fireball, it can readily be concluded that the probability of electron-neutral collisions within this plasma structure is very small. Furthermore, the mean free path increases with decreasing electron temperature, which makes also the energy transfer between the cold electrons and neutrals even more unlikely. The order of magnitude of the mean free path for electrons with kinetic energies of around 1.5 eV lies on the order of 50 cm and more in our experiments.[15] Hence, the assumption of isothermal electrons, which holds in our case only for the low temperature electrons, is in direct contradiction with the explanation of neutral gas heating via electron-neutral collisions. The mean free path, on the other hand, of ion-neutral collisions is much smaller, and thus, neutral gas heating just outside the FB via inelastic ion-neutral collisions is far more likely.

IV. CONCLUSION AND OUTLOOK

The theory of force exertion by plasma fireballs has been generalized to FBs with non-thermal electrons. This was done due to the discrepancy between the assumptions of existing analytical models and the available experimental data. The model proposed in this paper describes the shape of the electron density and the radial plasma potential profile very accurately. It has been shown that the potential drop, which is predicted for the double layer around such a FB, is considerably larger than expected before. Due to this finding, it becomes possible to argue that the primary heating processes of neutrals by the FB are rather induced by collisions between accelerated ions that gain sufficient energy in the potential drop of the FB anode. This claim is also corroborated by the fact that the large collision mean free path between electrons and neutrals is too large to play a significant role in the gas heating. The total force and the ion flux through the FB surface were calculated based on the model herein, and it was found that the force exerted by FB with non-isothermal electrons is considerable. These results offer an interesting possibility for the technical applications of fireballs as it suggests their potential use for space propulsion as this force was achieved with a total input power of 130 W including the power for producing the background plasma in the linear machine. Furthermore, most modern thruster systems working with gases with high atomic mass like krypton or xenon are very cost intensive and require input powers on the order of several kW.[16,17] It has been shown in this work that plasma FBs are capable of producing substantial thrust at very little input power and in low mass gases such as Ar. The concept of using double layers for space propulsion is not a new one. The so-called Hall double layer thrusters (HDLTs) were described, for example, in the work of Charles.[18] FB assisted thrusters offer, in principle, the same advantages as HDLTs like the lack of movable parts which leads to a longer lifetime or the possibility to operate the device in the steady state and in the pulsed mode. Moreover, FBs produce additional ions very efficiently within the rather large potential drop of the surrounding sheath. Those ions enhance the overall thrust, but it has to be mentioned that the ion flow outwards the FB is spatially isotropic due to the spherical geometry. Hence, future work should be dedicated to improve the ion transport in a preferable direction in order to enhance the achievable thrust even further. This could be done by introducing suitable magnetic fields or even asymmetric FB configurations. That the latter is feasible at least for inverted FBs was shown in a previous paper.[19] However, the available experimental data and theoretical modeling are somehow scarce. Thus, an enhanced fundamental understanding of these phenomena is needed to lead the way to a new generation of ion thrusters for space propulsion. However, the model presented in this paper is just a first attempt to generalize existing models of fireball dynamics, and it is not fully complete. Further improvements are expected by also taking kinetic effects into account, but this was out of the scope of this work and is left to future research.

[1]O. Lehmann, "Gasentladungen in weiten Gefässen," Ann. Phys. **312**(1), 1–28 (1902), ISSN 1521-3889.
[2]R. L. Stenzel, C. Ionita, and R. Schrittwieser, "Neutral gas dynamics in fireballs," J. Appl. Phys. **109**(11), 113305 (2011).
[3]G. Makrinich and A. Fruchtman, "The force exerted by a fireball," Phys. Plasmas **21**(2), 023505 (2014).
[4]S. M. Rubens and J. E. Henderson, "The characteristics and function of anode spots in glow discharges," Phys. Rev. **58**, 446–457 (1940).
[5]B. R. Weatherford, E. V. Barnat, and J. E. Foster, "Two-dimensional laser collision-induced fluorescence measurements of plasma properties near an

rf plasma cathode extraction aperture," Plasma Sources Sci. Technol. **21**(5), 055030 (2012).
[6]T. Gyergyek, M. Čerček, R. Schrittwieser, and C. Ionita, "Experimental study of the creation of a fire-rod i: Temporal development of the electron energy distribution function," Contrib. Plasma Phys. **42**(5), 508–525 (2002).
[7]T. K. Popov, P. Ivanova, M. Dimitrova, J. Kovačič, T. Gyergyek, and M. Čerček, "Langmuir probe measurements of the electron energy distribution function in magnetized gas discharge plasmas," Plasma Sources Sci. Technol. **21**(2), 025004 (2012).
[8]R. L. Stenzel, C. Ionita, and R. Schrittwieser, "Dynamics of fireballs," Plasma Sources Sci. Technol. **17**(3), 035006 (2008).
[9]M. A. Lieberman and A. J. Lichtenberg, *Principles Of Plasma Discharges And Materials Processing* (John Wiley & Sons, 2005).
[10]D. Levko and J. Gruenwald, "Influence on the emission current on a beam-generated plasma," Phys. Plasmas (submitted).
[11]F. Magnus and J. T. Gudmundsson, "Digital smoothing of the Langmuir probe I-V characteristic," Rev. Sci. Instrum. **79**(7), 073503 (2008).
[12]J. Annaloro, V. Morel, A. Bultel, and P. Omaly, "Global rate coefficients for ionization and recombination of carbon, nitrogen, oxygen, and argon," Phys. Plasmas **19**(7), 073515 (2012).
[13]A. V. Phelps, C. H. Greene, and J. P. Burke, Jr., "Collision cross sections for argon atoms with argon atoms for energies from 0.01 eV to 10 keV," J. Phys. B: At., Mol. Opt. Phys. **33**(16), 2965 (2000).
[14]J. R. Roth, *Industrial Plasma Engineering: Volume 2-Applications to Nonthermal Plasma Processing* (CRC Press, 2001), Vol. 2.
[15]G. Franz, *Low Pressure Plasmas and Microstructuring Technology* (Springer Science & Business Media, 2009).
[16]J. A. Linnell and A. D. Gallimore, "Efficiency analysis of a hall thruster operating with krypton and xenon," J. Propul. Power **22**(6), 1402–1418 (2006).
[17]R. R. Hofer, *Development and Characterization of High-Efficiency, High-Specific Impulse Xenon Hall Thrusters* (University of Michigan, 2004).
[18]C. Charles, "Plasmas for spacecraft propulsion," J. Phys. D: Appl. Phys. **42**(16), 163001 (2009).
[19]J. Gruenwald, J. Reynvaan, and P. Knoll, "Creation and characterization of inverted fireballs in H_2 plasma," Phys. Scr. **2014**(T161), 014006.